Vortex Dynamics in a Compact Kardar-Parisi-Zhang System

A. Zamora, N. Lad[ORCID], and M. H. Szymanska

Department of Physics and Astronomy, University College London, Gower Street, London WC1E 6BT, United Kingdom

We study the dynamics of vortices in a two-dimensional, nonequilibrium system, described by the compact Kardar-Parisi-Zhang equation, after a sudden quench across the critical region. Our exact numerical solution of the phase-ordering kinetics shows that the unique interplay between nonequilibrium and the variable degree of spatial anisotropy leads to different critical regimes. We provide an analytical expression for the vortex evolution, based on scaling arguments, which is in agreement with the numerical results, and confirms the form of the interaction potential between vortices in this system.

Topological defects play an important role in two-dimensional (2D) critical systems with either U(1) or SO(2) symmetry [1]. A paradigmatic example is the Berezinskii-Kosterlitz-Thouless (BKT) phase transition between disordered and ordered phases of the equilibrium planar XY model, caused by vortices binding at low temperatures due to their mutual attractive interactions [2,3]. Topological defects emerge naturally in a large number of *nonequilibrium* systems [4–7], although their roles at criticality are still largely unexplored. One paradigmatic case is the compact Kardar-Parisi-Zhang (cKPZ) equation [8,9], which appears as a natural extension of the noncompact KPZ equation, [10,11], when considering the compactness of the phase. The cKPZ equation has a wide range of physical applications from driven-dissipative condensates, such as microcavity polaritons [12–16], polar active smectic phases [17], transport phenomena in periodic media (driven vortex lattices in disordered superconductors [18,19]), and synchronization and frequency stability in networks and lattices of coupled limit-cycle oscillators to coupled optomechanical oscillators [20].

Recent theoretical studies suggest that the critical properties of 2D systems governed by the cKPZ equation differ substantially from their equilibrium counterparts, and that the BKT theory cannot be extended to all regimes [5,9,21]. This is rooted in the fact that the vortex-antivortex (V-AV) interactions in an isotropic or weakly anisotropic (WA) cKPZ system, in contrast to the equilibrium XY model, become repulsive beyond a characteristic length scale. In this scenario, a disordered vortex-dominated phase composed of unbound vortices emerges and precludes a phase transition to a quasiordered state in the thermodynamic limit. However, in the strongly anisotropic (SA) cKPZ system, the V-AV interaction is even more attractive than in the XY model, and, consequently, the bound vortex pairs stabilize a quasiordered phase at low noise levels, to some extent as in the BKT theory for equilibrium systems.

In this Letter, we present the first clear confirmation of these predictions, based on an exact numerical solution of the full cKPZ dynamics, following a rapid quench across the critical region. We explore the regime of parameters accessible to the mentioned analytical methods and beyond. We observe both (i) the new vortex-dominated disordered phase in the WA scenario and (ii) the quasi-ordered phase with diminishing number of V-AV pairs in the SA case. Finally, we complement our numerical study with an analytical derivation of the vortex equations of motion by considering scaling arguments and the approximate V-AV interaction potential, which is in excellent agreement with the numerics of the full cKPZ dynamics. This confirms that the approximate form of the vortex interactions captures the essential physics.

The cKPZ equation and the vortex interaction.—The cKPZ equation for compact variable $\theta(\mathbf{r}, t)$ reads [5,8]

$$\partial_t \theta(\mathbf{r}, t) = \sum_{i=x,y} \left\{ D_i \partial_i^2 \theta(\mathbf{r}, t) + \frac{\lambda_i}{2} [\partial_i \theta(\mathbf{r}, t)]^2 + \eta(\mathbf{r}, t) \right\},$$

(1)

where, θ may denote *the phase* of the condensate, of the charge-density wave order parameter, the displacement field in a polar active smectic system, the phase field of coupled limit-cycle oscillators. The diffusion constants D_x and D_y are positive and here taken to be 1, which can be obtained by an anisotropic rescaling of the lengths. The nonlinear parameters λ can be either positive or negative and capture the nonequilibrium nature of the system. The Gaussian noise term with zero mean fulfils $\langle \eta(\mathbf{r}, t) \eta(\mathbf{r}', t') \rangle = 2\sigma^2 \delta_{\mathbf{r}, \mathbf{r}'} \delta_{t, t'}$. Vortices in the system emerge as a consequence of the compactness of the θ variable in Eq. (1), since $\oint \nabla \theta d\mathbf{l} = 2\pi n(\mathbf{r}, t)$, with $n(\mathbf{r}, t) \in \mathbb{Z}$ [5], where $\mathbf{l}$ is the contour. Consequently, $n(\mathbf{r}, t) \neq 0$ denotes a vortex with charge n, at site $\mathbf{r}$ and time t.

As has been shown by Sieberer and coworkers [5,8,9], by considering the dual electrodynamical (dED) picture of the cKPZ equation and a perturbative expansion in the nonlinear parameters λ, the vortices in the cKPZ system interact through a force with both conservative and nonconservative contributions due to the nonequilibrium nature of the system; in contrast to the equilibrium XY model, i.e., when $\lambda_x = \lambda_y = 0$, where the vortices interact through only central Coulomb forces [22,23]. However, in the present study we are interested in the scaling and critical properties of the system and, consequently, in the interdistance R between a vortex and an antivortex in a pair. Thus, we consider only the central force within the vortex pair, which can be obtained from the V-AV potential $V(R)$ through $F_{va}(\mathbf{R}) = -\nabla V(R)$. This potential, for charge ± 1 vortices reads [5]

$$V(R) = \frac{1}{\epsilon}\log\left(\frac{R}{D_c}\right) - \frac{a}{3\epsilon^3}\log^3\left(\frac{R}{D_c}\right), \quad (2)$$

where ϵ is the dielectric constant of the nonlinear dED theory, D_c is the size of the vortex core, and $a \equiv 2\alpha_+^2 - (\alpha_-^2/2) + (\alpha_+\alpha_-/2)\cos(2\tilde\theta)$, with $\tilde\theta$ being the angle of the vortex-antivortex dipole, which is set to an average value of zero in the present study. The α coefficients are $\alpha_\pm = \lambda_\pm/(2D)$, with $\lambda_\pm = (\lambda_x \pm \lambda_y)/2$ and $D = D_x = D_y$. The first term of the potential (2) (zero order in λ's, i.e., $\lambda_+ = \lambda_- = 0$) coincides with the potential of the V-AV interaction in the planar XY model. The second term of Eq. (2) comes from the second order correction in the expansion in λ's. The first order correction in λ does not appear in Eq. (2) since it does not give a central contribution to the force [5,9].

Differently to the equilibrium case, where the V-AV interaction is always attractive, the potential (2) can give both attractive and repulsive contributions, depending on the relative sign of the nonlinearities λ [5,9]. Specifically, when both λ's have different signs, which defines the SA regime, the force between V and AV is always attractive and enhanced with respect to the analogous force in the equilibrium XY model. When the λ's have the same sign, which identifies the WA regime, the V-AV force is attractive only up to a given length scale L_v [obtained from the condition $F_{va}(\mathbf{R}) = 0$] beyond which it becomes repulsive [9,21]. For the isotropic case, where $\lambda_x = \lambda_y = \lambda$,

$$L_v = D_c \exp\left(2\sqrt{\epsilon}D/\lambda\right). \quad (3)$$

Consequently, it has been predicted that the steady-state of the system shows a vortex dominated phase, characterized by a nonzero density of repelling vortices with a mean interdistance L_v [9,21,24], also observed in the context of the complex Ginzburg-Landau equation [25].

Dynamical equation for the vortex density.— Considering the vortex potential (2) and general scaling arguments we derive a dynamical equation for the vortex

density ρ in the long range limit, which reproduces the numerical integration of the cKPZ equation (1), revealing that the dynamics of the vortices is governed by the conservative and central forces given by the potential (2). The starting point is to consider the dynamical equation for a single V-AV pair in the cKPZ system. Assuming that the central potential (2) leads to viscous-relaxation dynamics of the phase (where the forces coming from the central potential are compensated by friction forces on each vortex [26,27]), for a V-AV pair: $F_{va} + 2F_\mu = 0$, where $F_\mu = \mu v$ is the friction acting on a single moving vortex with velocity v and inverse mobility μ. Since $v = dD/dt$, where D is the distance between the vortex and antivortex, leads to [6,9,26,28]

$$2F_\mu = 2\mu(D)\frac{dD}{dt} = -F_{va}(D). \quad (4)$$

The crucial point for characterising the vortex dynamics is the form of μ since, as in the case of the XY model, we expect a nontrivial dependence on D. In this Letter we calculate μ associated with a single moving vortex with velocity $\mathbf{v}$ of modulus v, whose field configuration is given by ϕ_v. The frictional force reads as $F_\mu = -\nabla_\mathbf{v}(dE/dt)$, with $dE/dt = \int d^2\mathbf{r}(\delta H/\delta\theta)(d\theta/dt) = \int d^2\mathbf{r}(d\theta/dt)^2 = v^2\int d^2\mathbf{r}(\partial\phi_v/\partial_x)^2$ [27–29], where $E = \int d^2\mathbf{r}H$ is the total energy of the vortex configuration with energy density H. Consequently, $\mu = F_\mu/v \propto \int d\mathbf{r}(\partial\phi_v/\partial_x)^2 \approx \int d\mathbf{r}|\nabla\theta_0|^2$, for an isotropic vortex located at the origin in the zero-velocity limit, whose field is given by θ_0.

Finally, we calculate $\nabla\theta_0$ with the help of the dED relation $\nabla\theta_0 = z \times \mathbf{E}_0$ [8,9], where $\mathbf{E}_0 = -\nabla V_v(\mathbf{r})$ is the electrostatic field created by a single charge (vortex) located at the origin, and the potential $V_v(\mathbf{r})$ coincides with potential (2), since we are considering vortices with charge one. Therefore, we find that

$$\mu(r) \propto \left\{\log(\tilde r) - \frac{2}{3}\tilde a\log^3(\tilde r) + \frac{1}{5}\tilde a^2\log^5(\tilde r)\right\}, \quad (5)$$

where $\tilde r \equiv r/D_c$ and $\tilde a = a/\epsilon^2$. Expression (5) contains the characteristic $\log(\tilde r)$ dependence of the equilibrium XY model ($\lambda_x = \lambda_y = \tilde a = 0$) followed by higher logarithmic powers from the nonlinearity λ, characteristic of the KPZ system. We now derive the dynamical equation for the vortex density ρ by considering that the system in the long range limit is characterized by a unique single length scale ξ, a characteristic velocity $v_\xi = d\xi/dt$, and characteristic elastic $F_{va}(\xi)$ and viscous $\mu(\xi)d\xi/dt$ forces [26,27]. Taking an absolute value of Eq. (4) we obtain

$$\mu(\xi)\frac{d\xi}{dt} \propto \frac{1}{\xi}\left|1 - \tilde a\log^2\left(\frac{\xi}{D_c}\right)\right|, \quad (6)$$

which leads to the vortex density dynamics in the long range limit through the relation $\rho \sim 1/\xi^2$ and using Eq. (5).
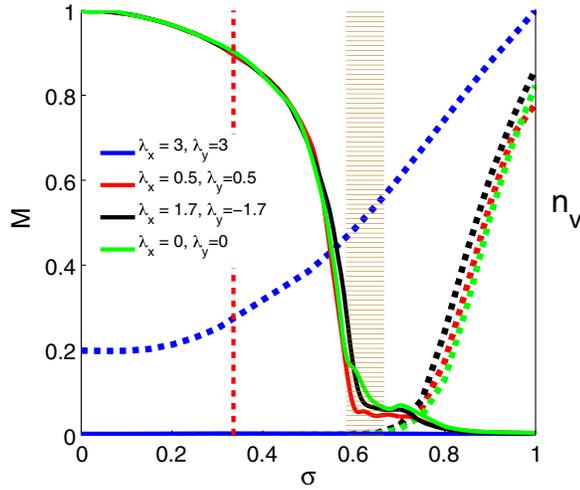
FIG. 1. Steady state of the cKPZ system. Steady-state density of vortices ρ (in arbitrary units, dashed curves) and magnetization M (solid curves) as a function of the noise parameter σ for different λ. The vertical dashed line indicates the final noise $\sigma_f = 1/3$ for the infinite rapid quench shown in Figs. 3 and 4. For the XY model with $\lambda = 0$ (green curves) and the SA case with $\lambda_x = -\lambda_y$ (black curves) the system exhibits (quasi)ordered and disordered phases separated by a critical noise $\sigma_c \approx 0.63$ (striped rectangle). However, for the isotropic case with large nonlinearity λ (blue curves), the system shows a vortex-dominated phase with no magnetization even at low noise values.

Vortex dynamics after an infinitely rapid quench.—Here, we study the dynamics of the vortex density after an infinitely rapid quench from a completely disordered phase to a low noise regime with $\sigma_f = 1/3$ [see Fig. 1] by exact numerical solution of full cKPZ equation (1). Phase ordering kinetics following this type of quench protocol has been used to study universal properties of both equilibrium [26,27,30–32] and nonequilibrium [33,34] complex systems.

Steady state.—Before addressing the quench dynamics, we first characterize the nonequilibrium steady state (Fig. 2). We find that in the SA regime, characterized by different signs of λ_x and λ_y, the system shows two distinct phases in the steady state: (i) A phase with vanishing density of vortices at low noise levels below a critical noise σ_c (left panel in Fig. 2); and with a finite magnetization $M^2(t) = (1/V_s)(m_x^2 + m_y^2)$, where V_s is the volume of the system, $m_x = \langle \int d^2\mathbf{r} \cos\theta(\mathbf{r}, t)\rangle$, $m_y = \langle \int d^2\mathbf{r} \sin\theta(\mathbf{r}, t)\rangle$, and $\langle \cdots \rangle$ denotes averaging over stochastic realisations. Note that M depends slightly on λ. (ii) A disordered phase, characterized by a high density of vortices, which destroy the magnetization at noise levels above σ_c. This critical behavior shown in Fig. 1, equivalent to the one present in the equilibrium XY model ($\lambda_x = \lambda_y = 0$), is consistent with analytical predictions by Sieberer *et al.* using approximate methods [5].

However, this picture changes completely at the WA regime, i.e., λ_x and λ_y with the same sign. We find that the
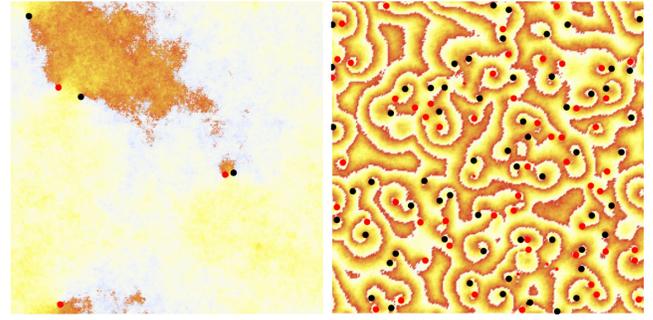
FIG. 2. $\theta(\mathbf{r})$ at late times with marked vortices. 2D maps with position of vortices (black dots) and antivortices (red dots) on top of the $\theta(\mathbf{r})$ profile for a single realisation in two different regimes: (i) phase ordering configuration in the SA regime with $\lambda_x = -\lambda_y = 1.7$ (left panel), note that due to periodic boundaries the red V at the bottom is paired with the black AV on the top, and (ii) vortex-dominated phase for $\lambda_x = \lambda_y = 1.5$ in the isotropic regime (right panel). Note that the left panel shows the whole system, whereas the right panel shows a zoomed quarter (see the plot for the whole system in Fig. 8 of the Supplemental Material [35]).

steady state shows a nonzero density of topological defects, which destroy the magnetization, even at low and vanishing noise levels when $\lambda \geq 2.5$, with $\lambda = \lambda_x = \lambda_y$ (see Fig. 1 and right panel of Fig. 2). The transition between a (quasi) ordered phase and disordered phases is gone. We obtain that the density of vortices is independent of the noise at low noise strengths, revealing the length scale expressed in Eq. (3) [35], which is a clear indicator of the vortex dominated phase predicted by Sieberer *et al.* [5,9], and analogous to one identified in the context of the complex Ginzburg-Landau equation [25]. We also observe that for low values of λ, the characteristic length L_v exceeds the system size considered in this study and, consequently, the system does not exhibit the vortex dominated phase. In contrast, it shows two distinct phases as in the SA case, one with a finite M and low vortex density (at low noise levels) and another with a high density of entropic vortices, which destroy the magnetization of the system (see the $\lambda_x = \lambda_y = 0.5$ case in Fig. 1). This behavior is a finite size effect since $L_v > L$ in this case, where L is the system size.

Diffusive decay of the vortex density.—First, we consider an infinitely rapid quench through a critical point in the SA regime for different cases. Our exact numerical solutions of the cKPZ equations show that the vortex density decays in time following a diffusive law with a logarithmic correction as in the equilibrium XY model, i.e., $\rho \sim [\log(t)/t]^\alpha$ [27,31], as we can see in Fig. 3. (for further details of the fit and discussion we refer to Fig. 7 and Secs. II and IV of Supplemental Material [35]). An example of late time dynamics for $\lambda_x = -\lambda_y = 1.7$ case is shown in the left panel of Fig. 2 for a configuration with 3 pairs of vortices and in Fig. 8 of the Supplemental Material [35] for a configuration with no vortices. There is a very good agreement between
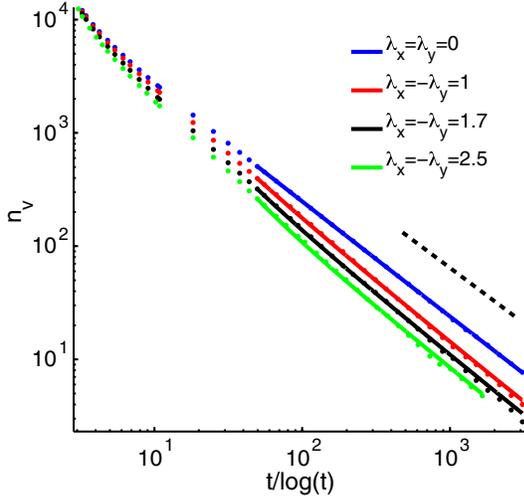
FIG. 3. Vortex dynamics in the SA regime. Number of vortices n_v as function of time $t/\log(t)$ after a sudden quench from a high noise disordered initial state to a low noise σ_f final state. The dots show the numerical solution of the KPZ equation and the solid lines the theoretical prediction from Eq. (6). We observe a diffusive law with a logarithmic correction: $n_v \sim [\log(t)/t]^\alpha$, with $\alpha \approx 1$ for all the different configurations. Specifically $\alpha = 1.016 \pm 0.010, 1.111 \pm 0.011, 1.130 \pm 0.015, 1.142 \pm 0.015$ from top to bottom [35]. The dashed line shows the $\alpha = 1$ case.

FIG. 4. Vortex dynamics in the WA regime. Number of vortices n_v as a function of time $t/\log(t)$ after a sudden quench from a disordered initial state to a low noise σ_f final state. The dots are from the numerical solution of the cKPZ equation and the solid lines are the analytical estimate from Eq. (6). From top to bottom: $\lambda = 3.5, 3.25, 3.0, 2.75, 2.5, 2.25, 1.9, 0.5$, with $\lambda \equiv \lambda_x = \lambda_y$. We observe a saturation of the number of vortices at $\rho_S(\lambda)$ for $\lambda \geq 1.9$, which is a clear indicator of the vortex-dominated phase [35]. Inset: Blue dots show the characteristic length scale $L_v \sim \rho_S^{-1/2}$ obtained from numerics and red solid line from the expression (3) for $2.5 \leq \lambda \leq 4.0$.

the vortex dynamics coming from our numerics and the dynamics predicted by Eq. (6). For all values of λ considered here, the exponent $\alpha \approx 1$ (the difference between the values of the exponents for the $\lambda \neq 0$ and the $\lambda_x = \lambda_y = 0$ is less than 15%. We, however, notice a weak dependence of the exponent α on λ with α for $\lambda \neq 0$ being close to 1.1 [35]. It is not clear whether this deviation from $\alpha = 1$ is due to the nonuniversal corrections, which could be attributed to the enhancement of the V-AV interaction when increasing λ, or whether the system falls into a different universality class with a critical exponent $\alpha = 1.1$ rather then $\alpha = 1$. This will require further investigations.

Vortex-dominated phase.—The isotropic system shows a completely different behavior. First, for low values of $\lambda \equiv \lambda_x = \lambda_y$, the decay of the vortex density scales asymptotically with the inverse time $\rho \sim 1/t^\beta$. In contrast to the SA case, the exponent β can be much smaller than 1 and depends strongly on λ (see, for example, the $\lambda = 0.5$ case in Fig. 4). Note, that again the theoretical prediction of the dynamics of the vortices given by Eq. (6) is in very good agreement with numerical solutions of the cKPZ equation, as displayed in Fig. 4. Specifically, we observe that β decreases sharply when increasing λ, and becomes $\beta \approx 0$ for $\lambda \geq 1.5$, which indicates that the system reaches a steady state with a nonzero density of vortices ρ_S (see the right panel of Fig 2 where we can observe the distinctive spiral configuration of the V-AV phase as predicted in Ref. [5]). We believe that this saturation in the vortex

density is a consequence of the repulsive interactions between the Vs and AVs in the isotropic and WA regime at large distances. The characteristic length scale we obtain from the numerical simulations through $\rho_S \sim 1/L_v^2$ [21] (the inset panel of Fig. 4) agrees extremely well with the theoretical exponential dependence on $1/\lambda$ [5,9] derived in Fig. 4 [35] and so indicates the emergence of the disordered vortex dominated phase. Finally, we should stress that the lack of saturation in the number of vortices for the $\lambda = 0.5$ case is a finite size effect, i.e., the length scale associated with the inverse of the steady-state vortex density exceeds the size of the system considered in the present work. We expect a saturation of the number of vortices for all values of λ for an infinite system.

Summary and outlook.—We have explored the crucial role of topological defects in the critical behaviour of a nonequilibrium system described by the cKPZ equation by determining numerically the full dynamics after a sudden quench through a critical point. We have also derived an analytical expression for the vortex density dynamics, using the approximate form of the vortex–antivortex potential [5], which is in excellent agreement with the numerical results.

Crucially, in the isotropic or WA KPZ regime, i.e., when there are nonvanishing nonlinear terms of the same sign in both spatial directions, we have identified a phase characterized by a saturation of the vortex density in the phase ordering process. This novel behavior, with no counterpart in equilibrium systems, arises in the nonequilibrium scenario due to the external drive and dissipation, and can be

strongly modified by spatial anisotropy. We believe that this vortex dominated phase appears as a consequence of the repulsive V-AV interactions at large distances. Our results confirm the existence of a new vortex-dominated phase in systems larger then a characteristic length scale, which is exponentially dependent on the inverse of the nonlinear KPZ parameter.

In the opposite scenario, i.e., with either vanishing nonlinear terms or with no linearities of opposite sign in the two spatial direction (SA regime), we find that the vortex density decays in time algebraically with an exponent close to -1 and logarithmic corrections due to the attractive V-AV interactions, as in the equilibrium planar XY model scenario.

Since the cKPZ equation describes the behavior of a wide range of atomic, molecular and optical systems, it would be of a great interest to obtain the parameters of this equation from microscopic analysis of a particular realisation. This would allow us to determine whether the new vortex dominated phase as well as the transition between isotropic or WA and SA regimes can be practically realized in any of these realistic scenarios. Finally, the impact of the sign of the V-AV interaction on the vortex dynamics when the system crosses a critical point by following a *finite* quench has not yet been explored. This type of critical dynamics, which is successfully described for equilibrium systems by the Kibble-Zurek mechanism [40,41], can have different properties out of equilibrium, and is not to date clear whether the extension of the concept of adiabaticity could be carried over to the nonequilibrium scenarios [42,43].

[1] A. Altland and B. D. Simons, *Condensed Matter Field Theory* (Cambridge University Press, Cambridge, England, 2010).

[2] J. M. Kosterlitz and D. J. Thouless, J. Phys. C **6**, 1181 (1973).

[3] J. Kosterlitz, J. Phys. C **7**, 1046 (1974).

[4] K. Kawasaki, Ann. Phys. (N.Y.) **154**, 319 (1984).

[5] L. M. Sieberer and E. Altman, Phys. Rev. Lett. **121**, 085704 (2018).

[6] C. Reichhardt and C. J. O. Reichhardt, Rep. Prog. Phys. **80**, 026501 (2016).

[7] S. P. Thampi, R. Golestanian, and J. M. Yeomans, Europhys. Lett. **105**, 18001 (2014).

[8] L. M. Sieberer, G. Wachtel, E. Altman, and S. Diehl, Phys. Rev. B **94**, 104521 (2016).

[9] G. Wachtel, L. M. Sieberer, S. Diehl, and E. Altman, Phys. Rev. B **94**, 104520 (2016).

[10] M. Kardar, G. Parisi, and Y. C. Zhang, Phys. Rev. Lett. **56**, 889 (1986).

[11] I. Corwin, Random Matrices Theory Appl. **01**, 1130001 (2012).

[12] E. Altman, L. M. Sieberer, L. Chen, S. Diehl, and J. Toner, Phys. Rev. X **5**, 011017 (2015).

[13] A. Zamora, L. M. Sieberer, K. Dunnett, S. Diehl, and M. H. Szymańska, Phys. Rev. X **7**, 041006 (2017).

[14] L. He, L. M. Sieberer, E. Altman, and S. Diehl, Phys. Rev. B **92**, 155307 (2015).

[15] L. M. Sieberer, M. Buchhold, and S. Diehl, Rep. Prog. Phys. **79**, 096001 (2016).

[16] L. M. Sieberer, A. Chiocchetta, A. Gambassi, U. C. Täuber, and S. Diehl, Phys. Rev. B **92**, 134307 (2015).

[17] L. Chen and J. Toner, Phys. Rev. Lett. **111**, 088701 (2013).

[18] I. S. Aranson, S. Scheidl, and V. M. Vinokur, Phys. Rev. B **58**, 14541 (1998).

[19] L. Balents, M. C. Marchetti, and L. Radzihovsky, Phys. Rev. B **57**, 7705 (1998).

[20] R. Lauter, A. Mitra, and F. Marquardt, Phys. Rev. E **96**, 012220 (2017).

[21] S. Diehl (private communication).

[22] P. Minnhagen, Rev. Mod. Phys. **59**, 1001 (1987).

[23] V. Ambegaokar, B. I. Halperin, D. R. Nelson, and E. D. Siggia, Phys. Rev. Lett. **40**, 783 (1978).

[24] V. Gladilin and M. Wouters, J. Phys. A **52**, 395303 (2019).

[25] I. S. Aranson, H. Chaté, and L.-H. Tang, Phys. Rev. Lett. **80**, 2646 (1998).

[26] B. Yurke, A. N. Pargellis, T. Kovacs, and D. A. Huse, Phys. Rev. E **47**, 1525 (1993).

[27] A. Bray, A. Briant, and D. Jervis, Phys. Rev. Lett. **84**, 1503 (2000).

[28] A. Bray, Phys. Rev. E **62**, 103 (2000).

[29] H. Pleiner, Phys. Rev. A **37**, 3986 (1988).

[30] A. J. Bray, Adv. Phys. **51**, 481 (2002).

[31] A. Jelić and L. F. Cugliandolo, J. Stat. Mech. (2011) P02032.

[32] C. Godreche and J. Luck, J. Phys. A **33**, 9141 (2000).

[33] P. Comaron, G. Dagvadorj, A. Zamora, I. Carusotto, N. Proukakis, and M. Szymańska, Phys. Rev. Lett. **121**, 095302 (2018).

[34] M. Kulczykowski and M. Matuszewski, Phys. Rev. B **95**, 075306 (2017).

[35] See Supplemental Material at http://link.aps.org/supplemental/10.1103/PhysRevLett.125.265701 for further details on the numerical methods used in this Letter, which includes Refs. [36–39].

[36] V. Miranda and F. Reis, Phys. Rev. E **77**, 031134 (2008).

[37] A. Greiner, W. Strittmatter, and J. Honerkamp, J. Stat. Phys. **51**, 95 (1988).

[38] K. Moser, J. Kertész, and D. Wolf, Physica (Amsterdam) **178A**, 215 (1991).

[39] D. Higham, X. Mao, and A. Stuart, SIAM J. Numer. Anal. **40**, 1041 (2002).

[40] T. W. Kibble, J. Phys. A **9**, 1387 (1976).

[41] W. H. Zurek, Nature (London) **317**, 505 (1985).

[42] P. Hedvall and J. Larson, arXiv:1712.01560.

[43] A. Zamora, G. Dagvadorj, P. Comaron, I. Carusotto, N. P. Proukakis, and M. H. Szymańska, Phys. Rev. Lett. **125**, 095301 (2020).